



Advanced microscopy solutions for monitoring the kinetics and dynamics of drug–DNA targeting in living cells

R.J. Errington^{a,*}, S.M. Ameer-beg^b, B. Vojnovic^b, L.H. Patterson^c, M. Zloh^c, P.J. Smith^d

^aDepartment of Medical Biochemistry and Immunology, University of Wales College of Medicine, Cardiff, CF14 4XN, UK

^bAdvanced Technology Development Group, Gray Cancer Institute, Mount Vernon Hospital, Northwood, Middlesex, UK

^cDepartment of Pharmaceutical and Biological Chemistry, The School of Pharmacy, University of London, London WC1N 1AX, UK

^dDepartment of Pathology, University of Wales College of Medicine, Cardiff, CF14 4XN, UK

Received 8 April 2004; accepted 5 August 2004

Available online 21 September 2004

Abstract

Many anticancer drugs require interaction with DNA or chromatin components of tumor cells to achieve therapeutic activity. Quantification and exploration of drug targeting dynamics can be highly informative in the rational development of new therapies and in the drug discovery pipeline. The problems faced include the potential infrequency and transient nature of critical events, the influence of micropharmacokinetics on the drug–target equilibria, the dependence on preserving cell function to demonstrate dynamic processes in situ, the need to map events in functional cells and the confounding effects of cell-to-cell heterogeneity. We demonstrate technological solutions in which we have integrated two-photon laser scanning microscopy (TPLSM) to track drug delivery in subcellular compartments, with the mapping of sites of critical molecular interactions. We address key design concepts for the development of modular tools used to uncover the complexity of drug targeting in single cells. First, we describe the combination of two-photon excitation with fluorescence lifetime imaging microscopy (FLIM) to map the nuclear docking of the anticancer drug topotecan (TPT) at a subset of DNA sites in nuclear structures of live breast tumor cells. Secondly, we demonstrate how we incorporate the smart design of a two-photon ‘dark’ DNA binding probe, such as DRAQ5, as a well-defined quenching probe to uncover sites of drug interaction. Finally, we discuss the future perspectives on introducing these modular kinetic assays in the high-content screening arena and the interlinking of the consequences of drug–target interactions with cellular stress responses.

© 2004 Elsevier B.V. All rights reserved.

Keywords: Minor groove ligands; Two-photon; Drug–target; Fluorescence lifetime imaging microscopy; Cell-based assays; Topotecan; DRAQ5

* Corresponding author. Tel.: +44 29 20746472; fax: +44 29 20744905.

E-mail address: erringtonrj@cardiff.ac.uk (R.J. Errington).

Contents

1. Introduction	154
1.1. Drug and molecular probe design	154
1.2. Mechanisms of action	155
1.3. Drug resistance pathways	155
2. Fluorescent bioactive drugs	155
2.1. Minor groove binders with fluorescent signatures	155
2.2. Topotecan, a fluorescent anticancer agent	156
3. Mapping subcellular localization of bioactive drugs	156
4. Single-cell time-lapse microscopy	157
5. Two-photon ‘dark’ DNA binding probes as quenching tools	157
5.1. Rationale behind the design of quenching agents	158
5.2. DRAQ5 properties and localization	159
5.3. DRAQ5 molecular modeling reveals both AT intercalation and docking at the minor groove	159
5.4. Monitoring drug quenching using DRAQ5	160
6. Fluorescence lifetime imaging microscopy (FLIM)	161
6.1. Recording fluorescence intensity as a function of time	161
6.2. Lifetime maps for topotecan	161
6.3. Combined quenching with lifetime mapping to reveal bound drug in the nucleus	162
7. Microscopy solutions to interface pharmacokinetic activity and pharmacodynamic response	163
7.1. Linking multiscale responses	163
7.2. Multiplexing assays to link stress induction with drug uptake at the single-cell level	163
8. High-throughput screening for enhancing the drug discovery process	164
9. Conclusion	165
Acknowledgements	165
References	165

1. Introduction

DNA is a significant target for a wide range of pharmacologically active agents not least many of the drugs deployed in anticancer therapy. A wide range of molecular interactions and target modifications is possible with critical events often involving the minor groove. Indeed, drugs that bind within the DNA minor groove are of considerable interest for their antimicrobial and antitumor activities, providing an impetus to studies on the dynamics of interactions at the minor groove together with the development of tools to investigate critical events in the native environment of the living cell. There are three areas in which the study of minor groove binding (MGB) ligands (MGBLs) have raised considerable interest:

1.1. Drug and molecular probe design

The original X-ray analysis studies of Kopka et al. [1] of the complex of netropsin with a B-DNA

dodecamer revealed that the antitumor antibiotic was capable of binding within the minor groove, by displacing the water molecules of the spine of hydration with base specificity achieved not by hydrogen bonding but by close van der Waals contacts. Accordingly, polyamide drugs, such as netropsin, distamycin and their derivatives, can be inserted into a narrow B-DNA minor groove to form 1:1 complexes that can distinguish AT base pairs from GC [2]. Subsequent attempts to develop synthetic “lexitropsins”—molecules capable of reading any desired short sequence of DNA base pairs—have involved a wide range of compounds including epipodophyllotoxin, bithiazoles, acridines, anthraquinones, ellipticine, nitrosoureas, benzoyl mustards and nitrogen mustards [3]. In most of these cases, each of the individual components of the lexitropsin conjugate retain their modes of action as far as interaction with DNA, and therefore opening up the possibility of the minor groove interaction being a critical design feature in the

development of drugs with modified sequence selectivity.

1.2. Mechanisms of action

Understanding the mechanisms of action of MGBLs is important given the increasing knowledge of the role of DNA sequence and conformation recognition in the assembly of molecular complexes for replication, transcription, recombination and repair. Thus, DNA sequence-selective binding agents bearing conjugated effectors have potential applications in the diagnosis and treatment of cancers as well as providing probes for investigating the molecular biology of the cell [3]. An important step forward is the realization that a number of MGBLs interfere with the catalytic activities of the DNA topoisomerases, and there is evidence that in some cases, this may be a primary determinant of the cytotoxic action of the agent [4]. The type I and type II DNA topoisomerases are nuclear enzymes that regulate topological and conformational changes in DNA, critical to cellular processes such as replication, transcription, chromosome segregation and the efficient traverse of mitosis. For example, the identification of the MGB activity of the type I DNA topoisomerase poison class of camptothecins provides new insights into the mechanisms of enzyme trapping on DNA and the subsequent cytotoxic events as the ternary complex of DNA–drug–enzyme interacts with active DNA replication forks in S-phase of the cell cycle. Thus, there is considerable interest in topoisomerase I as a therapeutic target [5], not least due to the cell cycle specificity of the pharmacodynamic response and the potential for combination with other agents generating discrete effects in other cell cycle phases.

1.3. Drug resistance pathways

This overriding issue is a major problem limiting the effectiveness of initially active anticancer agents. Resistance can arise from cellular or subcellular pharmacokinetic reasons, changes in target sensitivity or availability and not least in the effector pathways for drug responses. Active drug efflux transporters of the ATP binding cassette (ABC)-superfamily of proteins have a major impact on the pharmacological behavior of most of the drugs in use today [6]. For

example, the MDR1 (ABCB1) gene product, P-glycoprotein, is a membrane protein functioning as an ATP-dependent exporter of xenobiotics from cells. Its importance was first recognized because of its role in the development of multidrug resistance (MDR) of cultured tumor cells against various anticancer agents, but it also has critical function in normal tissues such as the brain, kidneys, liver and intestines. Early studies recognized the potential for MGBLs to act as substrates for drug efflux mechanisms [7,8].

An MGBL target DNA topoisomerase I relaxes supercoiled DNA by the formation of a covalent intermediate in which the active-site tyrosine is transiently bound to the cleaved DNA strand. The antineoplastic agent camptothecin and its derivatives specifically target DNA topoisomerase I, and several mutations, have been isolated that render the enzyme camptothecin-resistant [9]. Interestingly, there may be other discrete mechanisms of drug resistance associated with MGBL that have yet to be fully characterized. The discovery of an enhanced process for the ejection of the MGBL, Hoechst 33342, from the DNA [10] of cells with selective resistance to MGBLs [11,12] highlights the need to understand the dynamics of DNA–ligand interaction in live cells.

Advanced microscopy solutions in the study of the spatial and temporal aspects of the drug–target interactions in live cells can address issues in each of the interest areas discussed above. Analysis at the single-cell level addresses the problems of inherent heterogeneity observed in many biological systems. Early studies on MGBL or anticancer drug–DNA interactions often exploited the convenient fluorescent signatures and spectral characteristics of the agents [13–15].

2. Fluorescent bioactive drugs

2.1. Minor groove binders with fluorescent signatures

Many bioactive molecules, particularly those comprising linked ring structures, have chromophores capable of fluorescence excitation and therefore offer the possibility for tracking target interactions through methods such as monitoring steady-state fluorescence intensity, fluorescence quenching and fluorescence lifetime measurements. The *bis*-benzimidazole dyes or

Hoechst probes, for example, have been extensively used to determine DNA content and nuclear morphology in fixed cell preparations [16]. They also cross the plasma membrane of living cells and bind to the minor groove. Absorbance occurs at UV wavelengths with a broadband emission spectrum ranging from 420 to 600 nm, dependent on dye–base pair ratios. These agents show impressive fluorescence spectral properties with two-photon excitation (using femto-second pulses from a Ti:sapphire laser) between 830 and 885 nm [17]. Recently, high-resolution studies have applied two-photon standing wave fluorescence photobleaching to understand the diffusive motion of DNA-containing chromatin in live cells [18].

2.2. Topotecan, a fluorescent anticancer agent

Several major classes of anticancer agents and their metabolites have fluorescence signatures including those agents that target enzyme–DNA complexes comprising DNA topoisomerases I or II. Topotecan (TPT) consists of a five-ringed structure (10-[(dimethylamino) methyl]-4-ethyl-4,9-dihydroxy-1*H*-pyrano[3',4':6,7]indolizino[1,2-*b*]quinoline-3,14-[4*H*,12*H*]-dione monohydrochloride); it is a UV-excitabile camptothecin and these autofluorescent properties have been exploited to evaluate drug resistance in differentially derived cell lines using confocal microscopy [19]. TPT molecule is an extended molecule and therefore has some of the key features of a good two-photon absorbing fluorophore [20], enabling symmetrical charge transfer from one end of the molecule to the middle, and vice versa. TPT displays a high two-photon cross-section near 25 GM for wavelengths within the range of a Ti:Sapphire laser (700–880 nm) and previous studies have shown that it is possible to detect the drug at micromolar concentrations in plasma [21].

TPT acts specifically by binding to the topoisomerase I–DNA complex [22]. The action of the agent arises from DNA replication forks encountering drug-stabilized cleavable complexes, generating cytotoxic double-strand breaks in the DNA that interfere with cell cycle progression resulting in cell death by apoptosis [23]. An important implication for the current study is that Streltsov et al. [24] have also shown that TPT binds to DNA, probably at the minor groove.

We have employed TPT as a “candidate” drug to exemplify the concepts of dynamic tracking of drug interactions with intracellular targets in live breast tumour cells (MCF-7). In this current article, we show how the use of two-photon laser scanning microscopy (TPLSM) [25,26] approaches to trace the uptake and delivery of drug to cellular compartments, and to map the drug binding to DNA–target sites with fluorescence lifetime imaging microscopy (FLIM).

3. Mapping subcellular localization of bioactive drugs

Pharmacokinetic maps reflecting inherent cell–cell heterogeneity for TPT drug delivery within a population of human breast tumour MCF-7 cells were acquired using TPLSM. To confirm previous spectroscopy studies that TPT can be detected using two-photon excitation, a concentration of 10 μ M of free TPT was added to cultures seeded in a coverslip observation chamber, and single optical sections collected using TPLSM at 790 nm and fluorescence emission collected between 460 and 630 nm. Initial experiments with MCF-7 cells showed that after a 10-min exposure to TPT that the fluorescent signal in the extracellular medium is high with good signal-to-noise. A striking feature of the observations on the TPT loading of MCF-7 cells was the innate heterogeneity within the population. Two-photon excitation of MCF-7 single cells exposed to TPT showed significant variation in the intracellular fluorescence levels even after 10-min exposure (Fig. 1A, B). This heterogeneity was seen with significant numbers of cells demonstrating a persistent ability to maintain low drug levels. However, this level of drug is not sustained in the cell, and after 2 h, the detectable amount of drug (fluorescence) has fallen significantly (Fig. 1C, D). The bioactivity of topotecan reduces over time as hydrolysis occurs in the medium; this process is driven by physiological pH conditions of 7.2 [27]. As the active drug fraction in the extracellular space (medium) diminishes, the cellular levels also decrease because the hydroxy–acid form cannot cross the plasma membrane. Regardless of the absolute level of TPT uptake, the nucleus always appeared brighter than the cytoplasm and indeed based on a threshold intensity, it was possible to segment out this nuclear

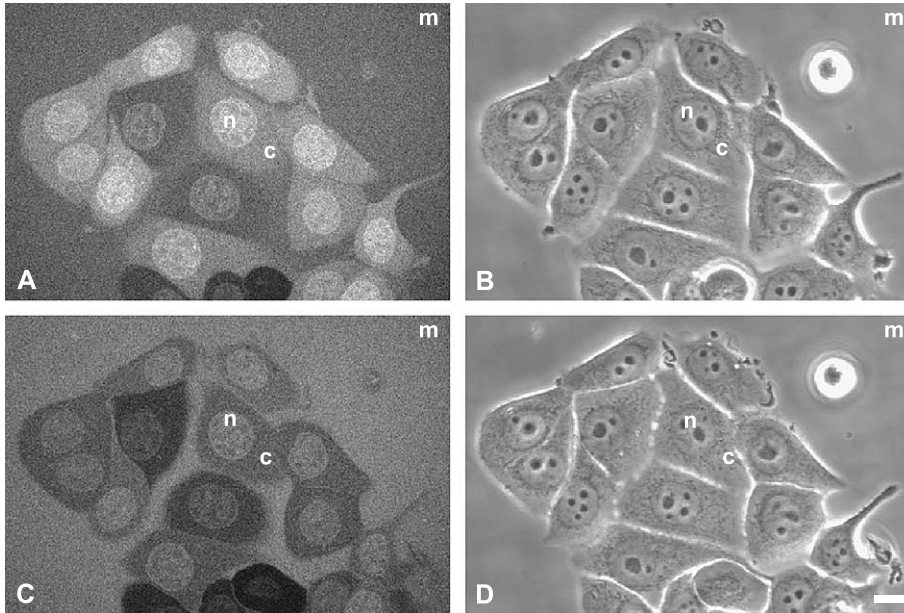


Fig. 1. Two-photon mapping of topotecan localisation in living cells. Cellular compartmentalisation in MCF-7 breast tumour cells: n, nucleus; c, cytoplasm; m, medium. (A) Peak uptake is achieved after 10 min and the culture demonstrates cell–cell heterogeneity. (B) Corresponding phase image. (C) At 60 min, the absolute levels of topotecan in each cell diminishes as the levels of active drug (membrane-penetrating) in the medium decreases. (D) Corresponding phase image. Bar is 10 μm .

compartment. Contrary to previous investigations, there was no obvious compartmentalisation in perinuclear organelles [28].

4. Single-cell time-lapse microscopy

Multicompartmental tracking of TPT uptake and washout kinetics in single cells provides a route for screening the dynamic process of drug delivery. The TPT uptake and delivery to the three cellular compartments (medium, cytoplasm and nucleus) was monitored using time-lapse TPLSM. Optical sections were acquired at an interval rate of 4.5 s (Fig. 2A). The presence of TPT fluorescence in the extracellular medium immediately became detectable post-addition and the cells appeared negatively stained. Each cell increased in fluorescence intensity over the emerging time course up to a total period of 500 s. The images (Fig. 2A) represent typical drug localization and progress of signal increase within the heterogeneous population. Once the drug levels reach a maximum in the cells, the process was reversed with an immediate washout, by exchanging

with fresh medium (Fig. 2B). The time course showed an initial rapid efflux from the cellular compartment at approximately eightfold the initial uptake rate. However, the second phase becomes much more protracted with trace amounts ($<4 \mu\text{M}$) of drug still remaining in the nucleus after 10 min. Graphical plots enable us to parametrize these data to extract unique fluorescent signatures reflecting the heterogeneity for the population (Fig. 2B).

5. Two-photon ‘dark’ DNA binding probes as quenching tools

Pharmacokinetic characterization of an MGBL requires assays which incorporate informative molecular tools and conceptually the strategy for drug discovery and fluorescent probe discovery are the same. Therefore, a molecular modeling approach can be implemented to search for MGBL quenching agents with defined DNA binding and spectral properties. Quenching assays provide a unique means for dissecting subresolution molecular interactions.

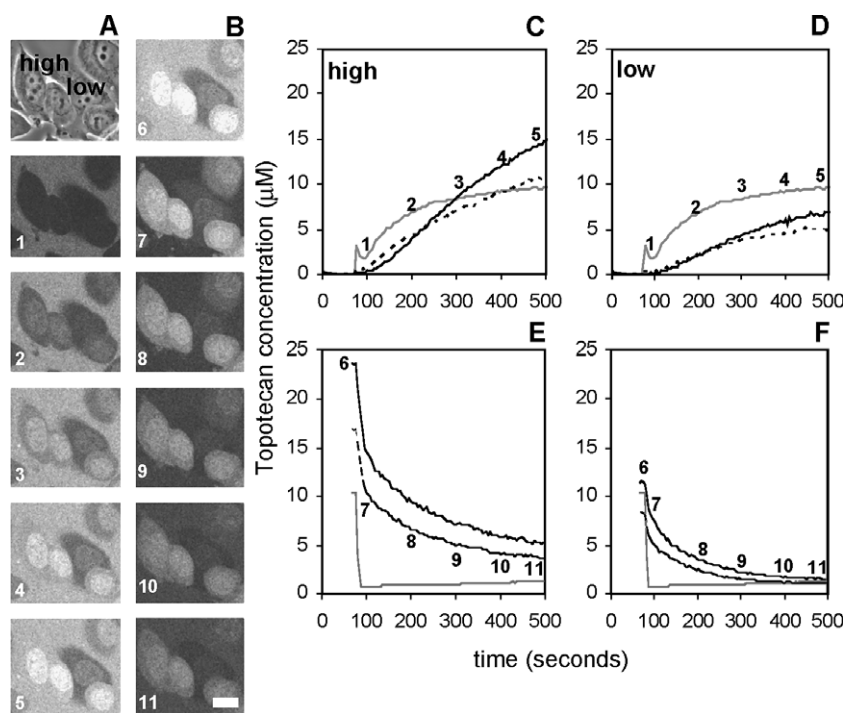


Fig. 2. Two-photon time-lapse microscopy to map cellular micropharmacokinetics. (A) A pulse of 10 μM topotecan was added to the medium (m) and the cells monitored for drug levels over 500 s. (B) Topotecan was removed instantaneously and drug efflux tracked for 500 s. (C and D) Graphical representation of drug uptake from low and high loading cells (as marked). (E and F) Corresponding washout kinetics for the same fields. The image time course is indicated on the graphs. Grey, medium; solid, nucleus; dotted, cytoplasm. Bar is 10 μm .

5.1. Rationale behind the design of quenching agents

The loss of fluorescent signal due to the occurrence of a second molecular event, which acts to reduce the photons emitted or indeed detected from a fluorescent probe or drug, can be termed as quenching; there are a variety of mechanisms which drive this process as a result of adding a quenching agent. Quenching usually results from collisions or complexes with solute molecules, reducing both the observed fluorescence lifetime and intensity via an increase in the nonradioactive decay from the excited state. Aromatic chromophores have radioactive lifetimes in the range of 1–100 ns, and therefore, the quenching rate must be rapid in order to be effective. Three main types of energy quenching occur in solution. The first, and most common, is collisional or dynamic quenching which occurs when a donor molecule in an excited singlet state collides with an acceptor resulting in energy transfer to this molecule rather than emission as a photon; this process is

clearly dependent upon the concentration of quencher. A second type of quenching occurs if the fluorophore and quencher form a ground (or excited) state complex that is weakly or nonfluorescent; this can be termed as destructive quenching. The third type of quenching occurs when two molecules have a close proximity to one another (less than 10 nm) and when the donor is excited, then static quenching can occur by a direct non-radioactive dipole–dipole transfer of energy to an acceptor which absorbs at the donor emission wavelength; fluorescent resonance energy transfer (FRET) exploits this latter type of quenching [29].

In the case of DNA tethering agents, another method of apparent quenching can be derived from molecular interactions, which do not involve energy transfer. The addition of a quenching agent which has similar binding properties to the fluorescent probe or drug could act to dislodge the fluorophore from the DNA, Hoechst 33258 and ethidium bromide are commonly used in fluorescent displacement assays

to study and determine the competitive docking of nonfluorescent DNA binding agents [30,31]. Finally, another approach is to add a DNA intercalating agent with a minimum potential for disassociation. In this manner, the agent could lock onto the DNA and perturb local chromatin structure, and hence acting as a “dislodging” probe for other DNA-associating molecules such as TPT.

Our design concept was to generate a multifaceted agent that established critical DNA binding properties as well as incorporating properties of a vital fluorescent probe. It was clear that it was important that the quenching agent should penetrate into living cells, and demonstrated spectral properties that ensured it was both detectable using fluorescence methods, but did not overlap with the TPT UV-fluorescent properties. The anthraquinones are a group of synthetic DNA affinity agents, structurally related to the DNA intercalating anthracycline antibiotics, and formed the basis of our search for useful TPT fluorescence quenching agents.

5.2. *DRAQ5 properties and localization*

We screened a range of substituted anthraquinones and selected the agent DRAQ5, a 1,5-*bis* {[2-(methylamino)ethyl]amino}-4,8-dihydroxy anthracene-9,10-dione. DRAQ5 showed an ability to bind to DNA in solution, penetrate the plasma membrane and to lock onto DNA in intact cells with high efficiency [32]. One-photon excitation at 647-nm wavelength, close to the $Ex_{\lambda_{max}}$, produced a fluorescence spectrum extending from 665 nm out to beyond 780 nm wavelengths. DRAQ5 appeared to achieve nuclear discrimination by its high affinity for DNA and did not show fluorescence enhancement with DNA in free solution. To obtain two-photon excitation of DRAQ5 on cellular DNA requires an IR wavelength in the region of 1047 nm, beyond that used to optimally excite TPT in these studies [33].

5.3. *DRAQ5 molecular modeling reveals both AT intercalation and docking at the minor groove*

Molecular modeling suggests that DRAQ5 is capable of binding to DNA through intercalation. The intercalation is stabilized by electrostatic interactions between the protonated tertiary amino group

of the side chain and the phosphate backbone of the DNA. Binding appears to involve a preference for AT-containing sequences [34] and that is confirmed by molecular modelling studies. *Ab initio* optimized geometries of DRAQ5 were docked into the DNA structures extracted from the PDB (protein data bank) files of the DNA complex with Hoechst 33342 (PDB access codes 127D, 129D, 303D). The docking was performed using global range molecular matching (GRAMM) software [35,36] and high-resolution rigid body searching for favorable binding configurations between a small ligand and a DNA without any constraints or limitations. Further modelling studies have shown that the aromatic moiety of DRAQ5 preferentially binds to the AATT part of the DNA sequence where Hoechst 33342 binds in the minor groove (Fig. 3A). Molecular dynamics simulation of the DNA–DRAQ5 complex without any constraints leads to DRAQ5 protrusion into the interface of two A–T pairs (Fig. 3B), by displacing the aromatic rings of two base pairs out of the DNA backbone and DRAQ5 stacking between those aromatic rings. In the second, slower stage, the DNA unwinds locally to create an intercalation site [37], which allows DRAQ5 to become fully inserted between aromatic rings of base pairs (Fig. 3C). The molecular modeling predicts that the macromolecular effects of adding DRAQ5 simultaneously with the drug TPT could effectively quench the fluorescent signal at the minor groove and AT-rich regions in nuclei.

To determine the efficiency with which DRAQ5 could act as an intranuclear fluorescence quenching agent on cellular DNA, we initially screened the ability of DRAQ5 to efficiently quench the fluorescence of the AT base pair-specific DNA minor-groove binding dye, Hoechst 33342. Dual beam flow cytometry showed that the levels of DRAQ5 signal were found to correspond closely with the disappearance of Hoechst 33342 signal. The removal of Hoechst 33342 from the medium prior to DRAQ5 addition did not affect the quench or anthraquinone uptake patterns observed, suggesting that DRAQ5 equilibrium across the plasma membrane was not affected by the presence of free Hoechst 33342 molecules. The findings are consistent with the ability of DRAQ5 to demonstrate AT base pair preferences when binding to DNA in living cells. Sequential imaging of dual-labelled samples generated staining

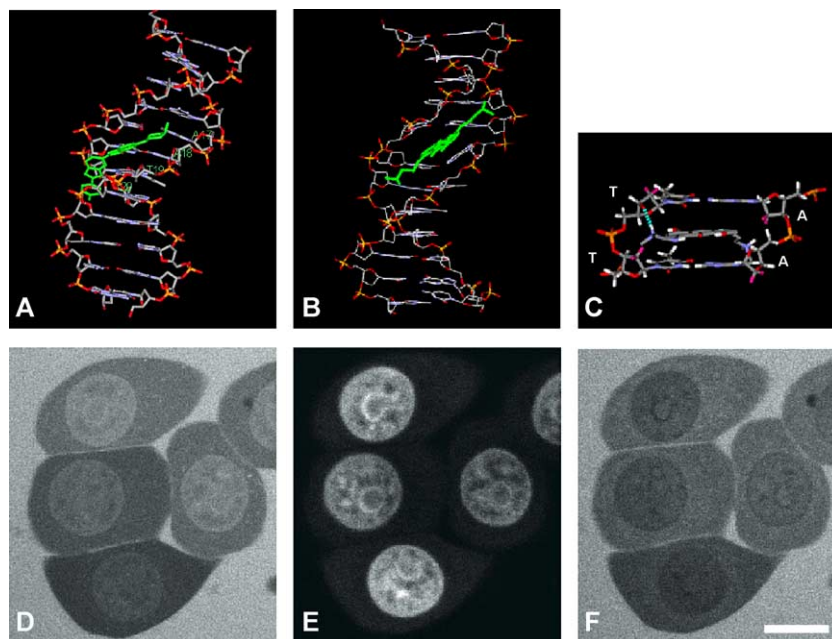


Fig. 3. Minor groove binding characteristics and implementation of the TPT quench probe, DRAQ5. (A) The docking of Hoechst into the minor groove of the DNA (CPK colour scheme). The position of the Hoechst was determined by X-ray crystallography (PDB access number 127D). (B) The energy minimized DNA-DRAQ5 complex after 100 ps of molecular dynamics simulation at 100 K. (CPK colour scheme). The position of DRAQ5 was found by rigid-body docking. (C) Model of structural orientation of DRAQ5 within intercalation site of the AT rich DNA sequence (hydrogen bond between protonated tertiary amino group and the phosphate backbone is depicted in cyan broken line). (D) High-resolution localisation map of TPT in MCF-7 cells using TPLSM. (E) DRAQ5 distribution 10 min post-addition. Image obtained using single-photon confocal LSM with excitation at 647 nm and detection using a 680/35-nm band pass emission filter. (F) Altered TPT localisation map. The quenched regions (no TPT signal) colocalise with the DRAQ5 positive signal. Bar is 10 μ m.

patterns derived from each probe in the same nucleus. The results showed that the fluorescence signals were colocalised immediately (within a few minutes), indicating extensive overlap of binding sites, before the Hoechst 33342 signal was titrated away as the concentration of DRAQ5 increased in the nucleus [34].

5.4. Monitoring drug quenching using DRAQ5

DRAQ5-induced TPT quenching was determined by the sequential imaging of two-photon excited TPT molecules at 790 nm wavelength (Fig. 3D) and single-photon activation of DRAQ5 (Fig. 3E) at 647 nm after 10 min. The results in Fig. 3 showed that the intracellular location of interphase nuclear DNA, given by the DRAQ5 fluorescence signal, corresponds to the intracellular location at which the TPT-signal is extinguished (Fig. 3F), without diminution of the

extracellular or cytoplasmic TPT signal (indicating that the effect is not due to the formation of an excited or ground state homodimer (at this concentration)). The culture continued to display intercellular heterogeneity, with overall fluorescence signal in the nucleus decreasing by 35%. Importantly, side-by-side imaging further showed that some of the topotecan fluorescence signal is not removed by this quenching agent, perhaps indicating that not all the binding sites of these two agents overlap. We would propose that both DRAQ5 and TPT could locate in close proximity (1–5 nm) to one another in the minor groove, enabling energy transfer and hence quenching. Although the complexity of the mechanism of quenching requires further clarification using spectroscopic studies and molecular modelling, this approach demonstrates that fluorescence–quenching using defined agents allows for the development of assays to reveal the molecular nature of DNA–drug interactions.

6. Fluorescence lifetime imaging microscopy (FLIM)

FLIM is a direct approach to monitoring all processes involving energy transfer between the fluorophore and the local environment [38], such as that which occurs when a fluorescent drug tethers to its DNA target [38,39]. Any energy transfer between the excited molecule and its environment changes the fluorescence lifetime in a predictable way.

6.1. Recording fluorescence intensity as a function of time

A recent implementation for recording fluorescence lifetime using a laser scanning microscope is by reverse start–stop time-correlated single-photon counting (TCSPC) [40,41]. Fluorescent molecules are excited using a pulsed laser source and the emission sampled by collection of single emitted photons. By measurement of the time between the detected fluorescence photon and the next laser pulse for many photon events, a probability distribution for the emission of a single photon, and thus the fluorescence decay curve, is estimated. Clearly, the assumption has to be made that much less than one photon is emitted per excitation event to recover the real probability distribution. We have used TPLSM multiplexed with time-correlated single-photon counting (TCSPC) to obtain combined intensity-lifetime images for determining TPT-DNA interactions in living cells. The system has been described elsewhere [42,43]; in brief, it comprises an ultrafast laser system coupled to an MRC1024 LSM modified with non-descanned single-photon counting photomultiplier detectors with good temporal performance. Photon pulses are routed to Becker and Hickl SPC700 TCSPC electronics with the reference signal derived from the laser via a fast photodiode. Pixel, line and frame clocks from the scanhead are used to record the three-dimensional photon density over the time and image coordinates. Cells were imaged with a 40× oil (1.3 NA Nikon Plan Fluor) for 300 s to acquire sufficient photon statistics for analysis. The SPC700 TCSPC system can accommodate count rates up to 1–2 MHz and are, therefore, able to record decay functions within a few milliseconds per pixel. This

method has a high-detection efficiency, a time-resolution limited only by transit time of the detector (i.e., pulse–pulse jitter and peak height variation), and directly delivers the decay function in the time domain. Previous spectroscopy studies have shown that binding of topotecan to DNA decamers d(AT)₁₀ considerably shortens the lifetime of TPT to 300 ps compared to 5.8 ns in an aqueous solution alone [44]. On this basis, we sought to map DNA–topotecan interactions in single cells.

6.2. Lifetime maps for topotecan

Least-square fitting of mono- and double-exponential decay analyses revealed the lifetime component(s) averaged for each pixel (128×128; Fig. 4A, B). In aqueous buffer (Hanks buffer at pH 7.2), the decays for 10 μM TPT 10 min after mixing were found to be monoexponential with a lifetime (τ) near 4.5 ± 0.68 ns. This remained unchanged during the course of 2 h, showing that FLIM measurements were not able to distinguish between active or inactive forms of the drug. Once inside the cell, TPT fluorescence decay still remained monoexponential but altered according to its compartmentalisation. The cytoplasmic lifetime (τ) was 4.0 ± 0.13 ns; however, in an additional perinuclear compartment (probably endoplasmic reticulum or mitochondria), the lifetimes were shortened to 3.5 ± 0.78 ns. The nucleus steady-state fluorescence intensity profile showed a complex distribution, with nuclear structures being highlighted. However, mean lifetime values in the nucleus of 4.2 ± 0.13 ns suggest that at equilibrium, the TPT is in an aqueous environment similar to that of the buffer. The lifetime distribution was similar in all regions of the nucleus independent of intensity values. Therefore, the intensity distribution we visualise in the nucleus, and indeed use to segment DNA structures, does not have a detectable short lifetime component under these conditions.

Previous studies have shown that when bound to DNA, the emission spectra of TPT is similar to that found in water [44]. This suggests that TPT exists in a highly polar environment when in the chromatin phase. We assume that the nuclear location comprises DNA-bound drug (i.e., to minor groove and topoisomerase I) and a larger pool of TPT in a chromatin aqueous phase. We suggest that the

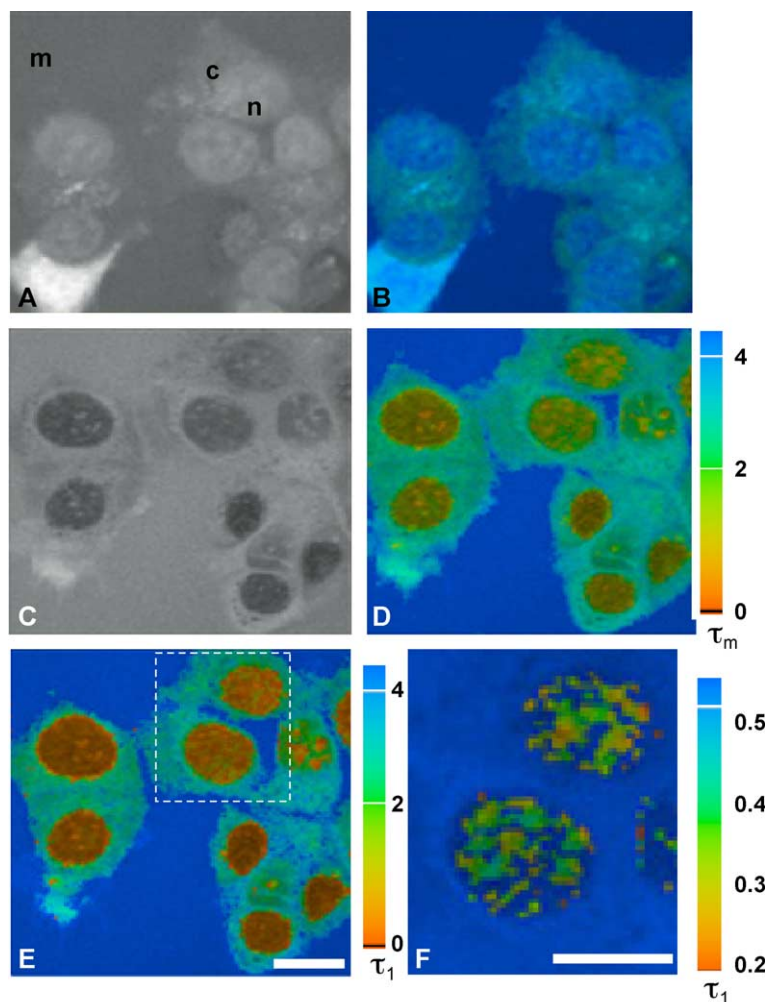


Fig. 4. Fluorescent lifetime maps to characterise TPT-target interactions. (A) Steady-state fluorescence intensity distribution 10 min after the addition of 2.5 μM TPT: n, nucleus; c, cytoplasm; m, medium. (B) Mean lifetime (τ_m) decay map (colour) fitted as a monoexponential combined with the intensity distribution (brightness). (C) Steady-state fluorescence intensity distribution 10 min after the addition of 2.5 μM TPT and with 20 μM DRAQ5 to quench the nuclear signal. (D) Mean lifetime map best fitted as a biexponential decay matrix. (E) Distribution map of the short-lifetime component (τ_1) representing TPT bound to target. (F) Zoomed nuclei of the same data as panel E with an altered look-up-table (LUT) to show the τ_1 (200–500 ps) values only. Bar is 10 μm and contrast wedge gives appropriate τ LUT (ns).

bound phase remains undetectable in this aqueous pool.

6.3. Combined quenching with lifetime mapping to reveal bound drug in the nucleus

DRAQ5 binds to DNA in the presence of TPT leading to apparent quenching of the fluorescent signal (Fig. 4C). We sought to determine the lifetime characteristics of the remaining signal in the nucleus.

The remaining, unmasked, signal is derived from a TPT-tethered component. In the medium, the fluorescence lifetime remains unchanged. The cellular compartments show much warmer colours indicating a drop in the mean lifetime, particularly in the nuclear compartment (Fig. 4D). In fact, in these cellular compartments, the best lifetime fit is derived from a biexponential model (by Chi square parameter and comparison of residuals). In order to reduce the uncertainty in determining the short lifetime compo-

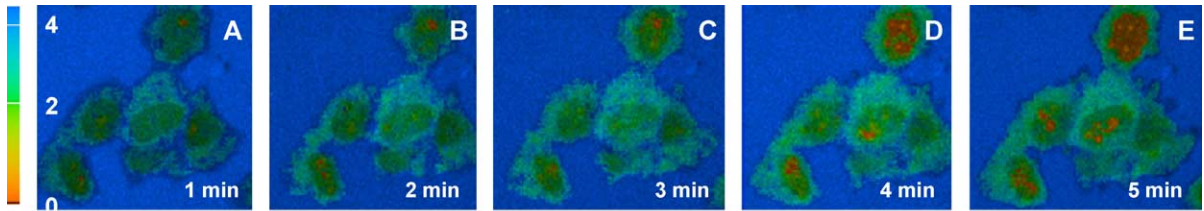


Fig. 5. Time-lapse FLIM to map the dynamic accumulation of bound TPT. Cells were pretreated for 5 min with DRAQ5 to quench DNA sites. A total of 2.5 μM TPT was added and 30-s FLIM snap-shots acquired over 5 min. (A–E) Total accumulation of drug over time is represented as brightness, while colour represents the increase in the short-lifetime component (τ_1). Bar is 10 μm and time is indicated on sequence.

ment, we determined the long lifetime component and assuming invariance of this component across the nucleus, the map of the bound short component (τ_1) becomes apparent and ranges from 310 to 510 ps, with an average amplitude of 75%, allowing to conclude that it is the predominant species in these nuclei. The punctuate pattern of a short lifetime component in the cytoplasmic compartment probably represents TPT compartmentalized in mitochondria.

Having verified that a readout signal was attainable representing bound drug, we tested the concept of acquiring time-lapse lifetime sequences to monitor the kinetic accumulation of bound drug within the nucleus. This was accomplished by prequenching the cells with DRAQ5, the acquisition time was reduced 10-fold to 30 s (Fig. 5). TPT entered in the cells as indicated by the pixel intensity and clusters of bound drug with a short lifetime component (τ_1) averaging at 390 ps, and accumulated in the nucleus. Because the two lifetime components can be determined *ab initio*, we can fix tau (τ) 1 and 2 to determine the time-dependent ratio of bound/unbound species and thereby elucidate the kinetics of binding to the unmasked target. Therefore, we have the capacity to monitor at a relatively high-temporal resolution the interaction of drug at target sites.

7. Microscopy solutions to interface pharmacokinetic activity and pharmacodynamic response

7.1. Linking multiscale responses

A significant challenge for the advancement of drug screening and evaluation is to link the biochemical and behavioural responses of genetically profiled

cells with the initial events of drug–target interaction. The efficiency and consequences of drug–target interaction can clearly be affected by pharmacokinetic factors but are also driven by parallel cellular events that are required to elicit the sought pharmacodynamic responses in a single cell. In understanding the pathways that determine the extent and nature of drug–target interaction, an important feedback loop for drug design concerns the linked cellular stress responses of a candidate agent. Significant advances in our understanding of the molecular mechanisms that follow the target-engagement of DNA damaging or cell cycle perturbing agents opens up an opportunity for developing interface assays which connect drug action and cell reaction.

7.2. Multiplexing assays to link stress induction with drug uptake at the single-cell level

The cellular response to TPT is driven by multiple factors, not least cellular pharmacokinetics and the corresponding population heterogeneity. A key question that arises from the previous sections is “to what extent does pharmacokinetic heterogeneity impose a mirrored pharmacodynamic response?” Here we exemplify an approach to address this issue by conducting the drug uptake assays using cultures grown on gridded coverslips or relocation substrates, and by monitoring drug uptake using TPLSM each cell is given a pharmacokinetic index as well as a coverslip coordinate. The coverslips are then processed to determine the expression of typical stress proteins such as the activation of p53 serine phosphorylation or increased p21^{waf1} levels [45–47]. The suggested action of TPT is to generate DNA damage through replicon collision with trapped topoisomerase I-DNA complexes that sequester single strand breaks

[48,49] and hence the anticancer agent is considered to be S-phase-specific. This implies that cancer cells that are not actively replicating DNA could resist the effects of the drug [46]. To correct the pharmacodynamic responses in S-phase and non-S-phase cells for the prevailing pharmacokinetic characteristics of an individual cell, we have tracked the consequences of TPT exposure in cells characterised for their nuclear concentration of TPT. Furthermore, to enhance the analysis, cells were also exposed to the S-phase-labelling agent BrdU [50] during the drug exposure,

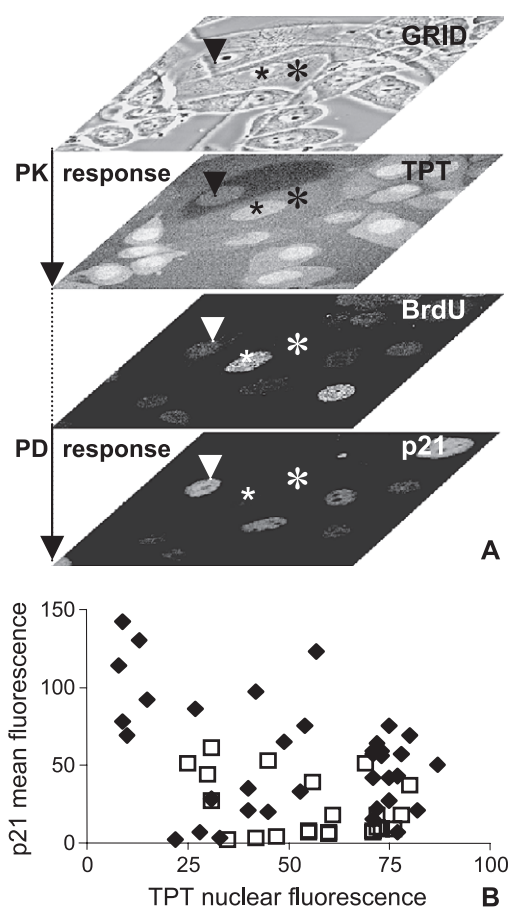


Fig. 6. Linking drug delivery with subsequent cellular stress responses. (A) Cells were grown on relocation coverslips (GRID). TPT was added together with BrdU (to mark replicating cells); drug levels were recorded for each cell (TPT). The slips were processed for immunofluorescence and the BrdU and p21^{waf1} levels assayed and coassigned a TPT level. (B) Cells were segmented as BrdU positive (□) or negative (◆).

thereby allowing cells that were actively engaged in DNA replication at the time to be identified. Probing for p21^{waf1} induction 6 h posttreatment at the single-cell level enabled us to demonstrate the phase-independent increase of expression and showed a distinct induction in both S-phase (BrdU positive) and non-S-phase cells (BrdU negative; Fig. 6A). Surprisingly, delivery of high levels of TPT to the nuclear compartment and active replication were not prerequisites for maximal stress induction in these breast tumour cells (Fig. 6B). Cell-based assays that attempt to report cell cycle-related events and targeting can be frustrated by the asynchronous nature of the cultures, cell-to-cell heterogeneity and the delayed kinetics with which a pharmacodynamic response may develop. We show that these problems can be addressed by the spatial and temporal connecting of events in single cells, even within heterogeneous cultures.

8. High-throughput screening for enhancing the drug discovery process

In order to meet the challenge of a rapidly increasing library of compounds within a drug discovery setting, and our growing understanding of emerging new cellular targets, the advanced assays described in this review need to be both sensitive and fast to work on high-throughput screening (HTS) imaging platforms. HTS calls for rigorous demands with respect to assay robustness and statistical accuracy. The current cellular imaging platforms commercially available are appropriate for both fluorescent kinetic and end-point read assays. The application of a confocal configuration confers axial spatial resolution bringing high-content screening to these platforms [51]. Previous investigations have applied multiphoton microscopy in a multiwell format and measured time-dependent intensity decays for a fluorescent MGBL 4' -6-diamidino-2-phenylindole (DAPI) [52]. Future perspectives on drug screening at the single-cell level leads to the requirement of miniaturised cell array biochip devices where the generation of candidate drugs is directly integrated or linked with the ability to perform on-line cell-based assays for drug–target interactions.

9. Conclusion

Drug design, discovery and deployment paradigms must progress from a situation where the cell system is an ill-defined and often homogenous “black-box” to an approach where the critical targets and molecular events within the cells become well-defined and provide spatially and temporally rich information. This ensures that drugs are not being rejected from a study because the signal-to-noise of a heterogeneous population is low, while in fact, the specificity or targeting of a drug is actually high (i.e., effective), but rare within that population. These are critical issues when concepts for therapy design of single- and multiple-agent anticancer drugs are being considered.

Advanced microscopy techniques now offer novel analytical tools and concepts. In terms of drug design, the evaluation of new agents and analogues in live cells fulfils the increasing demands of high-content screens aimed at improving the likelihood of identifying molecules with advantageous properties early on in the discovery cycle. Increasing our understanding of the mechanisms of action of important anticancer agents, focused around the molecular biology of the DNA topoisomerases, can now make use of the availability of tagged proteins and novel reporters to dissect the responses to target-trapping events. Furthermore, in the area of drug resistance, the development of tools for quantifying the contribution single or multiple pathways to a micropharmacokinetic profile offers both diagnostic tools for pathway expression and new means of evaluating resistance-reversing strategies.

Acknowledgements

The work was funded by grants awarded to PJS and RJE by UK Research Councils (GR/s23483), BBSRC (75/E19292), AICR (00-292) and SBRI (19666).

References

- [1] M.L. Kopka, C. Yoon, D. Goodsell, P. Pjura, R.E. Dickerson, The molecular origin of DNA-drug specificity in netropsin and distamycin, *Proc. Natl. Acad. Sci. U. S. A.* 82 (1985) 1376–1380.
- [2] M.L. Kopka, D.S. Goodsell, G.W. Han, T.K. Chiu, J.W. Lown, R.E. Dickerson, Defining GC-specificity in the minor groove: side-by-side binding of the di-imidazole lexitropsin to C-A-T-G-G-C-C-A-T-G, *Structure* 5 (1997) 1033–1046.
- [3] B.S. Reddy, S.K. Sharma, J.W. Lown, Recent developments in sequence selective minor groove DNA effectors, *Curr. Med. Chem.* 8 (2001) 475–508.
- [4] A.Y. Chen, C. Yu, B. Gatto, L.F. Liu, DNA minor groove binding ligands: a different class of mammalian DNA topoisomerase I inhibitors, *Proc. Natl. Acad. Sci. U. S. A.* 90 (1993) 8131–8135.
- [5] P.J. Smith, S. Soues, Multilevel therapeutic targeting by topoisomerase inhibitors, *Br. J. Cancer* 70 (1994) 47–51.
- [6] A.H. Schinkel, J.W. Jonker, Mammalian drug efflux transporters of the ATP binding cassette (ABC) family: an overview, *Adv. Drug Deliv. Rev.* 55 (2003) 3–29.
- [7] S.A. Morgan, J.V. Watson, P.R. Twentyman, P.J. Smith, Flow cytometric analysis of Hoechst 33342 uptake as an indicator of multi-drug resistance in human lung cancer, *Br. J. Cancer* 60 (1989) 282–287.
- [8] S.A. Morgan, J.V. Watson, P.R. Twentyman, P.J. Smith, Reduced nuclear binding of a DNA minor groove ligand (Hoechst 33342) and its impact on cytotoxicity in drug resistant murine cell lines, *Br. J. Cancer* 62 (1990) 959–965.
- [9] P. Fiorani, A. Bruselles, M. Falconi, G. Chillemi, A. Desideri, P. Benedetti, Single mutation in the linker domain confers protein flexibility and camptothecin resistance to human topoisomerase I, *J. Biol. Chem.* 278 (2003) 43268–43275.
- [10] P.J. Smith, M. Lacy, P.G. Debenham, J.V. Watson, A mammalian cell mutant with enhanced capacity to dissociate a *bis*-benzimidazole dye–DNA complex, *Carcinogenesis* 9 (1988) 485–490.
- [11] P.G. Debenham, M.B. Webb, Dominant mutation in mouse cells associated with resistance to Hoechst 33258 dye, but sensitivity to ultraviolet light and DNA base-damaging compounds, *Somat. Cell Mol. Genet.* 13 (1987) 21–32.
- [12] P.J. Smith, S.M. Bell, A. Dee, H. Sykes, Involvement of DNA topoisomerase II in the selective resistance of a mammalian cell mutant to DNA minor groove ligands: ligand-induced DNA–protein crosslinking and responses to topoisomerase poisons, *Carcinogenesis* 11 (1990) 659–665.
- [13] P.J. Smith, A. Nakeff, J.V. Watson, Flow-cytometric detection of changes in the fluorescence emission spectrum of a vital DNA-specific dye in human tumour cells, *Exp. Cell Res.* 159 (1985) 37–46.
- [14] P.J. Smith, H.R. Sykes, M.E. Fox, I.J. Furlong, Sub-cellular distribution of the anticancer drug mitoxantrone in human and drug-resistant murine cells analyzed by flow cytometry and confocal microscopy and its relationship to the induction of DNA damage, *Cancer Res.* 52 (1992) 1–9.
- [15] P.J. Smith, R. Desnoyers, L.H. Patterson, J.V. Watson, Flow cytometric analysis and confocal imaging of anticancer alkylaminoanthraquinones and their *N*-oxides in intact human cells using 647 nm krypton laser excitation, *Cytometry* 27 (1997) 43–53.

- [16] S.A. Latt, G. Stetten, L.A. Juergens, H.F. Willard, C.D. Scher, Recent developments in the detection of deoxyribonucleic acid synthesis by 33258 Hoechst fluorescence, *J. Histochem. Cytochem.* 23 (1975) 493–505.
- [17] F. Bestvater, E. Spiess, G. Stobrawa, M. Hacker, T. Feurer, T. Porwol, U. Berchner-Pfannschmidt, C. Wotzlaw, H. Acker, Two-photon fluorescence absorption and emission spectra of dyes relevant for cell imaging, *J. Microsc.* 208 (2002) 108–115.
- [18] S.K. Davis, C.J. Bardeen, The connection between chromatin motion on the 100 nm length scale and core histone dynamics in live XTC-2 cells and isolated nuclei, *Biophys. J.* 86 (2004) 555–564.
- [19] T. Litman, M. Brangi, E. Hudson, P. Fetsch, A. Abati, D.D. Ross, K. Miyake, J.H. Resau, S.E. Bates, The multi-drug-resistant phenotype associated with over-expression of the new ABC half-transporter, MXR (ABCG2), *J. Cell Sci., Suppl.* 113 (2000) 2011–2021.
- [20] T.G. Burke, H. Malk, I. Gryczynski, Z. Mi, J.R. Lakowicz, Fluorescence detection of the anticancer drug topotecan in plasma and whole blood by two photon excitation, *Anal. Biochem.* 242 (1996) 266–270.
- [21] M. Albota, D. Beljonne, J.L. Bredas, J.E. Ehrlich, J.Y. Fu, A.A. Heikal, S.E. Hess, T. Kogej, M.D. Levin, S.R. Marder, D. McCord-Maughon, J.W. Perry, H. Rockel, M. Rumi, G. Subramaniam, W.W. Webb, X.L. Wu, C. Xu, Design of organic molecules with large two-photon absorption cross sections, *Science* 281 (1998) 1653–1656.
- [22] C. Bailly, Topoisomerase I poisons and suppressors as anticancer drugs, *Curr. Med. Chem.* 7 (2000) 39–58.
- [23] C. Holm, J.M. Covey, D. Kerrigan, Y. Pommier, Differential requirement of DNA replication for the cytotoxicity of DNA topoisomerase I and II inhibitors in Chinese hamster DC3F cells, *Cancer Res.* 49 (1989) 6365–6368.
- [24] S.A. Streltsov, A.L. Mikheikin, S.L. Grokhovsky, V.A. Oleinikov, A.L. Zhure, Interaction of topotecan, DNA topoisomerase I inhibitor, with double-stranded polydeoxyribonucleotides: III. Binding at the minor groove, *Mol. Biol.* 36 (2002) 511–524.
- [25] W. Denk, J.H. Strickler, W.W. Webb, Two-photon laser scanning fluorescence microscopy, *Science* 248 (1990) 73–76.
- [26] N.S. White, R.J. Errington, Multi-photon microscopy: seeing more by imaging less, *Biotechniques* 33 (2002) 298–305.
- [27] I. Chourpa, J.M. Millot, G.D. Sockalingum, J.F. Riou, M. Manfait, Kinetics of lactone hydrolysis in antitumour drugs of camptothecin series as studied by fluorescence spectroscopy, *Biochem. Biophys. Acta* 1379 (1998) 353–366.
- [28] A.C. Croce, G. Bottiroli, R.E. Supino, V. Favini, Z. Zunino, Sub-cellular localisation of the camptothecin analogues, topotecan and gimatecan, *Biochem. Pharmacol.* 67 (2004) 1035–1045.
- [29] J.R. Lakowicz, *Principles of Fluorescence Spectroscopy*, 2nd edition, Plenum Press, 2003.
- [30] Y.H. Chen, Y. Yang, J.W. Lown, Design of distamycin analogues to probe the physical origin of the antiparallel side by side oligopeptide binding motif in DNA minor groove recognition, *Biochem. Biophys. Res. Commun.* 220 (1996) 213–218.
- [31] I.M. Johnson, S.G. Kumar, R. Malathi, De-intercalation of ethidium bromide and acridine orange by xanthine derivatives and their modulatory effect on anticancer agents: a study of DNA-directed toxicity enlightened by time correlated single photon counting, *J. Biomol. Struct. Dyn.* 20 (2003) 677–686.
- [32] M. Wiltshire, L.H. Patterson, P.J. Smith, A novel deep red/low infrared fluorescent flow cytometric probe, DRAQ5NO, for the discrimination of intact nucleated cells in apoptotic cell populations, *Cytometry* 39 (2000) 217–223.
- [33] P.J. Smith, N. Blunt, M. Wiltshire, T. Hoy, P. Teesdale-Spittle, M.R. Craven, J.V. Watson, W.B. Amos, R.J. Errington, L.H. Patterson, Characteristics of a novel deep red/infrared fluorescent cell-permeant DNA probe, DRAQ5, in intact human cells analyzed by flow cytometry, confocal and multiphoton microscopy, *Cytometry* 40 (2000) 280–291.
- [34] N. Marquez, S.C. Chappell, O.J. Sansom, A.R. Clarke, P. Teesdale-Spittle, R.J. Errington, P.J. Smith, Microtubule stress modifies intra-nuclear location of Msh2 in mouse embryonic fibroblasts, *Cell. Cycle* 3 (2004) 662–671.
- [35] E. Katchalski-Katzir, I. Shariv, M. Eisenstein, A.A. Friesem, C. Aflalo, I.A. Vakser, Molecular surface recognition: determination of geometric fit between proteins and their ligands by correlation techniques, *Proc. Natl. Acad. Sci. U. S. A.* 89 (1992) 2195–2199.
- [36] I.A. Vakser, Long-distance potentials: an approach to the multiple-minima problem in ligand–receptor interaction, *Prot. Eng.* 9 (1996) 37–41.
- [37] D. Graves, L.M. Velea, Intercalative binding of small molecules to nucleic acids, *Curr. Org. Chem.* 4 (2000) 915–929.
- [38] J.R. Lakowicz, I. Gryczynski, H. Malak, M. Schrader, P. Engelhardt, H. Kano, S.W. Hell, Time-resolved fluorescence spectroscopy and imaging of DNA labeled with DAPI and Hoechst 33342 using three-photon excitation, *Biophys. J.* 72 (1997) 567–578.
- [39] S.-I. Murata, P. Herman, J.R. Lakowicz, Texture analysis of fluorescence lifetime images of AT- and GC-rich regions in nuclei, *J. Histochem. Cytochem.* 49 (2001) 1443–1451.
- [40] D.V. O'Connor, D. Phillips, *Time-Correlated Single Photon Counting*, Academic Press, London, 1994.
- [41] A. Draaijer, R. Sanders, H.C. Gerritsen, Fluorescence lifetime imaging, a new tool in confocal microscopy, in: J.B. Pawley (Ed.), *Handbook of Biological Confocal Microscopy*, 2nd edition, Plenum Press, NY, 1995, pp. 491–505.
- [42] S.M. Ameer-Beg, P.R. Barber, R.J. Hodgkiss, R.J. Locke, R.G. Newman, G.M. Tozer, B. Vojnovic, J. Wilson, Application of multiphoton steady-state and lifetime imaging to mapping of tumour vascular architecture in vivo, *Proc. SPIE* 4620 (2002) 85–95.
- [43] S.M. Ameer-Beg, N. Edme, M. Peter, P.R. Barber, T.C. Ng, B. Vojnovic, Imaging protein-protein interactions by multiphoton FLIM, *Proc. SPIE* 5139 (2003) 180–189.
- [44] I. Gryczynski, Z. Gryczynski, J.R. Lakowicz, D. Yang, T.G. Burke, Fluorescence spectral properties of the anticancer drug topotecan by steady-state and frequency domain fluorometry

- with one-photon and multi-photon excitation, *Photochem. Photobiol.* 69 (1999) 421–428.
- [45] S. Houser, S. Koshlatyi, T. Lu, T. Gopen, J. Bargonetti, Camptothecin and zeocin can increase p53 levels during all cell cycle stages, *Biochem. Biophys. Res. Commun.* 289 (2001) 998–1009.
- [46] G.P. Feeney, R.J. Errington, M. Wiltshire, N. Marquez, S.C. Chappell, P.J. Smith, Tracking the cell cycle origins for escape from topotecan action by breast cancer cells, *Br. J. Cancer* 88 (2003) 1310–1317.
- [47] C. Tolis, G.J. Peters, C.G. Ferreira, H.M. Pinedo, G. Giaccone, Cell cycle disturbances and apoptosis induced by topotecan and gemcitabine on human lung cancer cell lines, *Eur. J. Cancer* 35 (1999) 796–807.
- [48] Y.H. Hsiang, L.F. Liu, Identification of mammalian DNA topoisomerase I as an intracellular target of the anticancer drug camptothecin, *Cancer Res.* 48 (1988) 1722–1726.
- [49] C. Kollmannsberger, K. Mross, A. Jakob, L. Kanz, C. Bokemeyer, Topotecan-A novel topoisomerase I inhibitor: pharmacology and clinical experience, *Oncology* 56 (1999) 1–12.
- [50] T. Porstmann, T. Temynck, S. Avrameas, Quantitation of 5-bromo-2-deoxyuridine incorporation into DNA: an enzyme immunoassay for the assessment of the lymphoid cell proliferative response, *J. Immunol. Methods* 82 (1985) 169–179.
- [51] L. Zemanova, A. Schenk, M.J. Valler, G.U. Nienhaus, R. Heilker, Confocal optics microscopy for biochemical and cellular high-throughput screening, *Drug Discov. Today* 8 (2003) 1085–1093.
- [52] J.R. Lakowicz, I.I. Gryczynski, Z. Gryczynski, High throughput screening with multi-photon excitation, *J. Biomol. Screen.* 4 (1999) 355–362.